

## Conformational Control of Chiral Amido-Thiourea Catalysts Enables Improved Activity and Enantioselectivity

Dan Lehnher, David D. Ford, Andrew J. Bendelsmith, C. Rose Kennedy, and Eric N. Jacobsen\*

Department of Chemistry and Chemical Biology, Harvard University, Cambridge, Massachusetts 02138, United States

## Supporting Information

**ABSTRACT:** While aryl pyrrolidinoamido-thioureas derived from  $\alpha$ -amino acids are effective catalysts in a number of asymmetric transformations, they exist as mixtures of slowly interconverting amide rotamers. Herein, the compromising role of amide bond isomerism is analyzed experimentally and computationally. A modified catalyst structure that exists almost exclusively as a single amide rotamer is introduced. This modification is shown to result in improved reactivity and



enantioselectivity by minimizing competing reaction pathways.

Dual hydrogen-bond (H-bond) donors, such as chiral urea and thiourea derivatives, have come to define an important class of catalysts for a range of highly enantioselective transformations.<sup>1</sup> Catalysts bearing the 2-aryl pyrrolidino amide motif have been of particular utility for promoting transformations via anion-binding or anion-abstraction pathways.<sup>2,3</sup> However, reactions enabled by these catalysts are frequently hampered by low efficiencies, requiring high catalyst loadings (5–20 mol %), long reaction times (>24 h), and/or dilute conditions ( $\leq 0.1$  M in initial substrate concentration) to achieve optimal results.

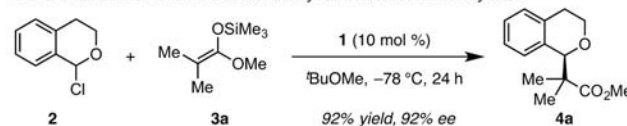
In an effort to elucidate the basis for these practical limitations to H-bond donor-mediated anion-abstraction catalysis, we recently reported a detailed mechanistic study of a representative transformation,<sup>4</sup> the enantioselective amido-thiourea-catalyzed alkylation of  $\alpha$ -chloroisochroman (**2**, Scheme 1A).<sup>3a</sup> This study revealed several key features of the reaction system, including: (1) The catalyst resting state under typical reaction conditions (0.1 M in substrate, 10 mol % of catalyst) is a nonproductive dimeric aggregate; (2) Two molecules of thiourea catalyst **1** are involved in the cooperative activation of the  $\alpha$ -chloroether electrophile; (3) Catalyst **1** exists as a mixture of slowly interconverting (*E*)- and (*Z*)-amide rotamers in solution (Scheme 1B).

Taken together, these observations imply that each of the pairwise combinations of the catalyst amide rotamers could participate in the alkylation transition state (*ZZ*-TS, *EE*-TS, *ZE*-TS, and *EZ*-TS)<sup>5</sup> and would likely make different, and potentially conflicting, contributions to the overall rate and enantioselectivity of the reaction. As such, we conjectured that constraining this catalyst system to operate through a single conformation could result in improved efficiency by funneling reactivity through a single enantioselective pathway. Herein we report the realization of this proposal through the mechanism-driven design and development of a conformationally biased catalyst that exhibits improved activity and enantioselectivity.

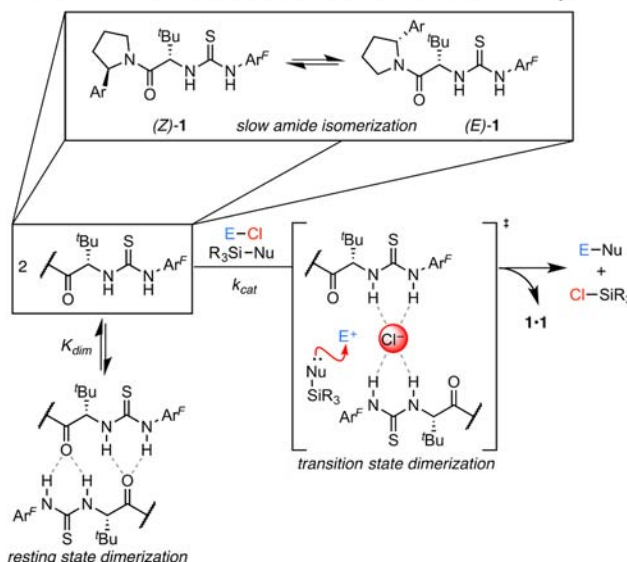
We sought first to identify the catalyst rotamer(s) responsible for controlling reactivity and enantioselectivity in the amido-

Scheme 1. Chiral Amido-Thiourea-Mediated Anion-Abstraction Catalysis<sup>a</sup>

## A. Enantioselective Amido-Thiourea-Catalyzed Oxocarbenium Alkylation



## B. General Mechanism for Amido-Thiourea-Mediated Anion-Abstraction Catalysis



<sup>a</sup>Ar<sup>F</sup> = 3,5-bis(trifluoromethyl)phenyl, Ar = 4-fluorophenyl, E = generic electrophile, Nu = generic nucleophile.

thiourea-catalyzed alkylation of  $\alpha$ -chloroisochroman (Scheme 1A). While only the (*Z*)-amide rotamer of catalyst **1** is observed in the solid state,<sup>6</sup> 1D and 2D <sup>1</sup>H NMR analysis provides

Received: May 17, 2016

Published: June 13, 2016

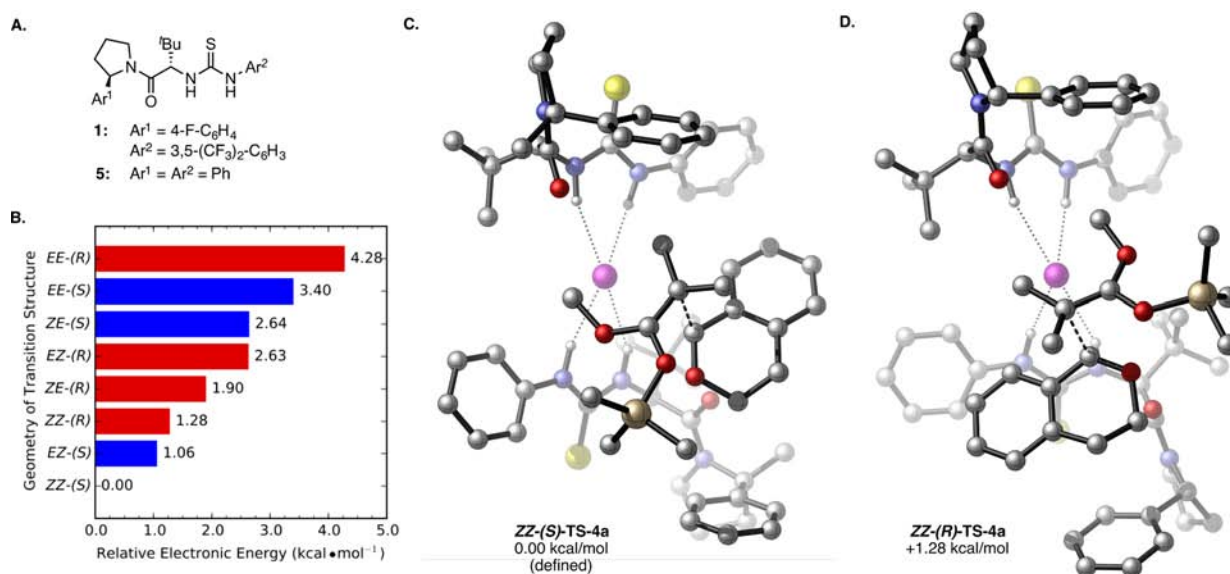
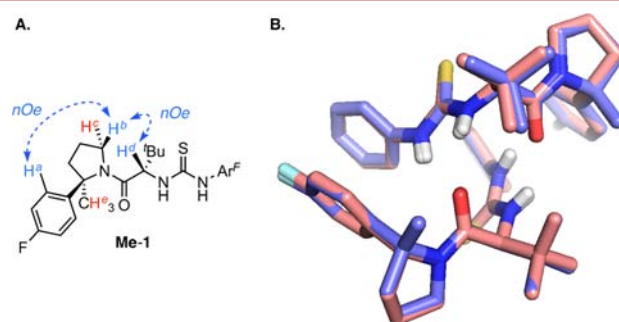


**Figure 1.** (A) Simplified catalyst **5** was utilized as a proxy for **1** in computational investigation. (B) A comparison of the relative energies of the lowest energy transition structures involving each of the four possible homodimeric and heterodimeric complexes of catalyst **5**. See ref **5**. Lowest energy computed transition structures involving the homodimeric (Z)-**5**/(Z)-**5** catalyst complex en route to the (C) major and (D) minor enantiomers of isochroman product **4a**. All calculations performed with B3LYP/6-31G+(d,p)//B3LYP/6-31G(d). Atom coloring scheme: C = silver, H = white, O = red, N = blue, S = yellow, Cl = magenta, Si = gold. Carbon-bound H atoms omitted for clarity.

evidence that (Z,Z), (Z,E), and (E,E) dimeric catalyst complexes all exist in solution.<sup>4a,c</sup> Density functional theory (DFT) calculations with simplified catalyst **5** (Figure 1A)<sup>7</sup> were employed to identify transition structures with each of the possible dimeric rotamer combinations.<sup>8,9</sup> Energetically accessible transition structures, each possessing a single imaginary frequency along the reaction coordinate, were located in all cases, lending credence to the hypothesis that multiple reaction pathways are competing under typical reaction conditions. Comparison of the transition structures en route to the major and minor enantiomers of product **4a** from each of the dimeric catalyst complexes (Figure 1B) revealed that the lowest energy structures (ZZ-(S)-TS-4a and ZZ-(R)-TS-4a) are accessed when both catalyst units are in the (Z)-conformation (Figure 1C,D).

Given these insights, we next sought to design an analogous catalyst scaffold that exists exclusively in the (Z)-rotameric form. The relative energies of the (E)- and (Z)-rotamers of amido-thiourea catalysts bearing a variety of substituents on the pyrrolidine moiety were determined computationally. From this analysis, the 2-aryl-2-methylpyrrolidine-derived amido-thiourea **Me-1** (Figure 2) was identified as a particularly promising candidate; this structure is predicted to favor the (Z)-amide rotamer by 2.8 kcal/mol. This energetic preference can be attributed to destabilizing *syn*-pentane interactions between the methyl substituent on the pyrrolidine and the amide  $\alpha$ -C–H bond in the (E)-amide conformation.<sup>10</sup> Furthermore, the optimized transition structure obtained with simplified catalyst **Me-5** is calculated to possess a very similar conformation to ZZ-(S)-TS-4a (vide infra).

In order to test these computational predictions, catalyst **Me-1** was prepared,<sup>11</sup> and its structural and functional properties were evaluated experimentally. Unlike catalyst **1**, only a single amide rotamer of **Me-1** can be observed by 1D <sup>1</sup>H and <sup>13</sup>C NMR in a variety of solvents. The structural assignment of the (Z)-amide rotamer was corroborated by 2D NOESY experiments in which diagnostic NOE correlations are observed (Figure 2A).

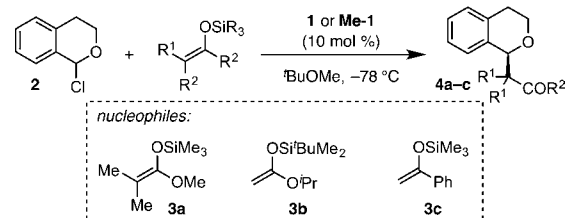


**Figure 2.** (A) Select NOE correlations utilized to assign **Me-1** as the (Z)-amide conformation. Correlations  $\text{H}^a \leftrightarrow \text{H}^b$  and  $\text{H}^b \leftrightarrow \text{H}^d$  are observed; correlations  $\text{H}^d \leftrightarrow \text{H}^e$  and  $\text{H}^c \leftrightarrow \text{H}^d$  are not. (B) Overlay of the H-bonded (Z)-**1**·(Z)-**1** (light pink) and **Me-1**·**Me-1** (slate blue) homodimeric complexes determined by X-ray crystallographic analysis. CF<sub>3</sub> groups and carbon-bound H atoms omitted for clarity.

Furthermore, the solid-state conformations of **1** and **Me-1** determined by single crystal X-ray diffraction analysis are nearly perfectly superimposable (Figure 2B).

The new thiourea derivative, **Me-1**, was evaluated in the model oxocarbenium alkylation reaction. This conformationally rigid catalyst was found to exhibit improved activity and enantioselectivity relative to **1**, affording **4a** with quantitative conversion in 97% ee after only 4 h (Table 1, entries 1 and 2).<sup>12</sup> Catalyst **Me-1** also displays a 2-fold rate enhancement relative to catalyst **1** for epimerization of  $\alpha$ -chloroisochroman-*d*<sub>3</sub> (Figure 3).<sup>4b,c</sup> This rate acceleration can be rationalized by the fact that (Z)-**1** and (E)-**1** exist in a 1:1 mixture under these conditions. If it is assumed that (E)-**1** is inactive in the epimerization process, then (Z)-**1** and **Me-1** can be concluded to display the same activity. This analysis lends credence to the assumption that **Me-1** operates through the same anion-abstraction mechanism elucidated to be operative with **1**.

In principle, the improved activity observed with catalyst **Me-1** could be due either to an increase in the effective concentration

**Table 1. Enantioselective Oxocarbenium Alkylation Enabled by Designed Catalyst Me-1<sup>a</sup>**


entry	nucleophile	time (h)	cat.	conv (%) <sup>b</sup>	ee (%)
1	3a	4	1	66	92 <sup>c</sup>
2			Me-1	>95	97 <sup>c</sup>
3	3b	1	1	81	85 <sup>d</sup>
4			Me-1	91	91 <sup>d</sup>
5	3c	24	1	82	88 <sup>d</sup>
6			Me-1	>95	96 <sup>d</sup>

<sup>a</sup>Reactions were run on 0.2 or 0.3 mmol scale and quenched after the designated time with 0.5 M NaOMe in MeOH. See ref 12.

<sup>b</sup>Conversion was determined from the relative integration of the <sup>1</sup>H NMR resonances of the product and quenched  $\alpha$ -methoxyisochroman.

<sup>c</sup>Determined by CSP–GC. <sup>d</sup>Determined by CSP–HPLC.

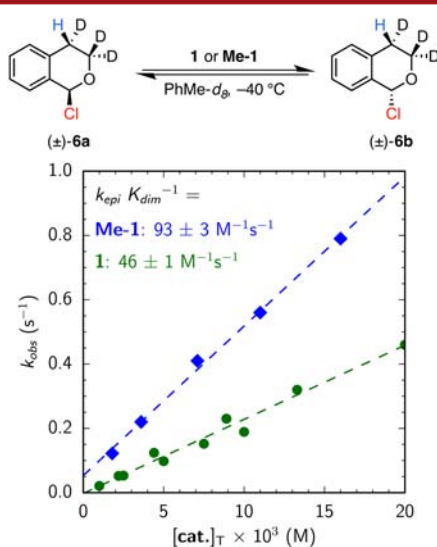


**Figure 3.** Observed first-order rate constant for epimerization of  $\alpha$ -chloroisochroman-*d*<sub>3</sub> (6) via anion abstraction catalyzed by **1** (green circles) or **Me-1** (blue diamonds). In all cases  $[6a] + [6b] = 0.10 \text{ M}$ .

of the active (Z)-rotameric form of the catalyst or to deaggregation of nonproductive ground state dimers. In order to differentiate between these possibilities, the self-dimerization equilibrium constants for catalysts **1** and **Me-1** were determined from the changes in the chemical shifts of diagnostic <sup>1</sup>H NMR signals observed upon serial dilution.<sup>13</sup> Catalyst **Me-1** was determined to possess a similar dimerization constant ( $K_{\text{dim}} = 3.1 \pm 0.1 \times 10^2 \text{ M}^{-1}$ ) to those determined for (E)- and (Z)-**1** ( $K_{\text{dim}} = 4.6 \pm 1.2 \times 10^2 \text{ M}^{-1}$  for (E)-**1** and  $K_{\text{dim}} = 2.0 \pm 0.3 \times 10^2 \text{ M}^{-1}$  for (Z)-**1**).<sup>14</sup> Thus, increased activity cannot be ascribed to selective deaggregation of the catalyst and must rather be attributed to the increased population of the more active (Z)-amide conformation.<sup>15</sup>

Similarly, the improved enantioselectivity could, in principle, be due either to minimization of competing pathways involving rotameric forms of the catalysts (as originally proposed) or to

intrinsically higher stereinduction imparted by introduction of the methyl substituent. These possibilities were distinguished by comparing the lowest energy transition structures for C–C bond formation located with catalysts (Z)-**5** and **Me-5** (B3LYP/6-31G+(d,p)//B3LYP/6-31G(d)). Catalyst methylation was found to have very little effect on the geometry of the transition structure leading to the major enantiomer of the product (Figure 1C; see Supporting Information for an overlay of the two computed structures), and the differential energy of activation was found to be similar between **Me-5** ( $\Delta\Delta E^\ddagger = 1.13 \text{ kcal/mol}$ ) and (Z)-**5**. ( $\Delta\Delta E^\ddagger = 1.28 \text{ kcal/mol}$ ).

These results suggest that improvement in the observed enantioselectivity with **Me-1** can be ascribed entirely to minimization of competing pathways involving the (E)-rotamer. This conclusion is corroborated by the observation that the enantioselectivity differences between catalysts **1** and **Me-1** are greatest under conditions in which the Z/E rotamer ratio of **1** is low.<sup>16</sup>

We anticipate that the conformational-control strategy outlined above will prove broadly beneficial in enantioselective anion-abstraction catalysis. For example, **Me-1** is found to be significantly superior to **1** in the alkylation of **2** with a silyl enol ether nucleophile (**3c**, Table 1, entries 5 and 6).

In conclusion, experimental and theoretical analyses have shed light on the detrimental role that catalyst amide rotamers play in anion-abstraction catalysis by aryl pyrrolidinoamido-thiourea derivatives. We have demonstrated the successful application of these mechanistic insights to the design of a new catalyst in which amide conformational control enables improved reaction efficiency and enantioselectivity. This design is likely to provide a general strategy for suppressing competing pathways in other transformations catalyzed by chiral amido-thioureas and related H-bond donor catalysts. The application of this design principle to development of highly efficient transformations is the focus of ongoing research.

## ■ ASSOCIATED CONTENT

### Supporting Information

The Supporting Information is available free of charge on the ACS Publications website at DOI: 10.1021/acs.orglett.6b01435.

Full experimental procedures, characterization data including NMR spectra for all new compounds, and geometries and energies of all calculated stationary points (PDF)

Crystallographic data for **Me-1** (CCDC 1477622 and 1478394), catalyst analogues (CCDC 1478392, 1478393, 1478395), and a synthetic intermediate en route to **Me-1** (CCDC 1477623) (CIF)

## ■ AUTHOR INFORMATION

### Corresponding Author

\*E-mail: jacobson@chemistry.harvard.edu.

### Notes

The authors declare no competing financial interest.

## ■ ACKNOWLEDGMENTS

This work was supported by the NIH (GM-43214) and by fellowships to D.L. (NSERC PDF), D.D.F. (Eli Lilly and Co.), and A.J.B. and C.R.K. (NSF DGE1144152). We thank Dr. Shao-Liang Zheng (Harvard X-ray Laboratory) for X-ray crystallo-



graphic structure determination and Erica D'Amato (Harvard University) for experimental assistance.

## REFERENCES

- (1) (a) Schreiner, P. R. *Chem. Soc. Rev.* **2003**, 32, 289–296. (b) Takemoto, Y. *Org. Biomol. Chem.* **2005**, 3, 4299–4306. (c) Doyle, A. G.; Jacobsen, E. N. *Chem. Rev.* **2007**, 107, 5713–5743. (d) Knowles, R. R.; Jacobsen, E. N. *Proc. Natl. Acad. Sci. U. S. A.* **2010**, 107, 20678–20685.
- (2) For reviews, see: (a) Zhang, Z.; Schreiner, P. R. *Chem. Soc. Rev.* **2009**, 38, 1187–1198. (b) Brak, K.; Jacobsen, E. N. *Angew. Chem., Int. Ed.* **2013**, 52, 534–561. (c) Phipps, R. J.; Hamilton, G. L.; Toste, F. D. *Nat. Chem.* **2012**, 4, 603–614. (d) Beckendorf, S.; Asmus, S.; Mancheño, O. G. *ChemCatChem* **2012**, 4, 926–936. (e) Seidel, D. *Synlett* **2014**, 25, 783–794.
- (3) For select examples, see: (a) Reisman, S. E.; Doyle, A. G.; Jacobsen, E. N. *J. Am. Chem. Soc.* **2008**, 130, 7198–7199. (b) Knowles, R. R.; Lin, S.; Jacobsen, E. N. *J. Am. Chem. Soc.* **2010**, 132, 5030–5032. (c) Birrell, J. A.; Desrosiers, J.-N.; Jacobsen, E. N. *J. Am. Chem. Soc.* **2011**, 133, 13872–13875. (d) Lin, S.; Jacobsen, E. N. *Nat. Chem.* **2012**, 4, 817–824. (e) Bergonzini, G.; Schindler, C. S.; Wallentin, C.-J.; Jacobsen, E. N.; Stephenson, C. R. J. *Chem. Sci.* **2014**, 5, 112–116. (f) Yeung, C. S.; Ziegler, R. E.; Porco, J. A., Jr.; Jacobsen, E. N. *J. Am. Chem. Soc.* **2014**, 136, 13614–13617. (g) Liu, R. Y.; Wasa, M.; Jacobsen, E. N. *Tetrahedron Lett.* **2015**, 56, 3428–3430.
- (4) (a) Ford, D. D.; Lehnher, D.; Kennedy, C. R.; Jacobsen, E. N. *J. Am. Chem. Soc.* **2016**, [10.1021/jacs.6b04686](https://doi.org/10.1021/jacs.6b04686). (b) Ford, D. D.; Lehnher, D.; Kennedy, C. R.; Jacobsen, E. N. *ACS Catal.* **2016**, [10.1021/acscatal.6b01384](https://doi.org/10.1021/acscatal.6b01384). (c) Ford, D. D. The Role of Catalyst-Catalyst Interactions in Asymmetric Catalysis with (salen)Co(III) Complexes and H-Bond Donors. Ph.D. Thesis, Harvard University, 2013.
- (5) The (E)-1 and (Z)-1 monomers in the heterodimeric catalyst complexes are conformationally inequivalent. Two distinct transition state classes are defined based on the orientation of each monomer relative to the reacting substrate. ZE-TS = Transition structures in which the amide oxygen of the (E)-1 monomer interacts with the oxocarbenium ion. EZ-TS = Transition structures in which the amide oxygen of the (Z)-1 monomer interacts with the oxocarbenium ion. See [Supporting Information](#) for additional information.
- (6) X-ray diffraction analysis of single crystals of **1** in the presence and absence of bound tetramethylammonium chloride enable assignment of dimeric structures of (Z)-1.
- (7) Catalyst **5** affords isochroman **4a** in 81% ee under standard reaction conditions and provides a significantly reduced computational cost relative to catalyst **1**.
- (8) Frisch, M. J.; et al. *Gaussian 09*, revision A.02; Gaussian, Inc.: Wallingford, CT, 2009; See [Supporting Information](#) for full citation.
- (9) (a) Becke, A. D. *J. Chem. Phys.* **1993**, 98, 5648–5652. (b) Lee, C.; Yang, W.; Parr, R. G. *Phys. Rev. B: Condens. Matter Mater. Phys.* **1988**, 37, 785–789. (c) Miehlich, B.; Savin, A.; Stoll, H.; Preuss, H. *Chem. Phys. Lett.* **1989**, 157, 200–206. (d) Frisch, M. J.; Pople, J. A.; Binkley, J. S. *J. Chem. Phys.* **1984**, 80, 3265–3269.
- (10) For a discussion of *syn*-pentane interactions in hydrocarbon backbones, see: Hoffmann, R. W.; Stahl, M.; Schopfer, U.; Frenking, G. *Chem. - Eur. J.* **1998**, 4, 559–566.
- (11) See [Supporting Information](#) for synthetic details.
- (12) These reactions were quenched with sodium methoxide after the indicated time to emphasize the rate enhancement achieved with **Me-1** versus **1**.
- (13) For discussion of this technique, see: (a) Tan, H. K. S. *J. Chem. Soc., Faraday Trans.* **1994**, 90, 3521–3525. (b) Nogales, D. F.; Ma, J.-S.; Lightner, D. A. *Tetrahedron* **1993**, 49, 2361–2372.
- (14) These values, which were determined in CD<sub>2</sub>Cl<sub>2</sub>, are in good agreement with the values determined previously in toluene-*d*<sub>8</sub>. See refs **4a** and **4c**.
- (15) See [Supporting Information](#) for discussion and data.
- (16) For example, in toluene at –78 °C, catalyst **1** exists as a 1:1 mixture of (Z)-1 and (E)-1 and affords **4a** in 76% ee. **Me-1** affords **4a** in 91% ee.